

TeVPA  
2023

 **ATLAS**  
EXPERIMENT

JG|U



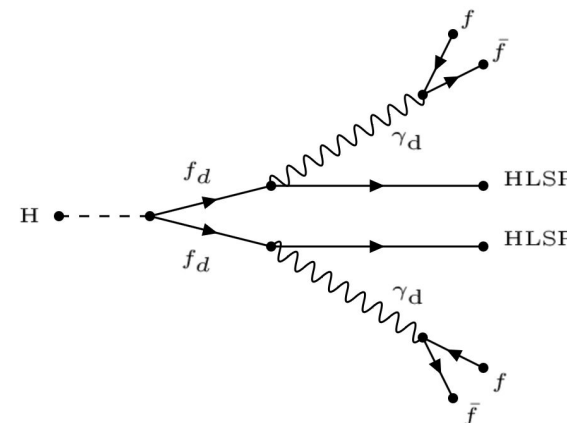
**Non-WIMP dark matter searches  
with the ATLAS detector**

Olivera Vujinović on behalf of the ATLAS  
Collaboration

- Overview of results of recent searches on the dark sector, dark photons, LLPs, ALPs, dark QCD, semi-visible jets obtained with data collected in  $pp$  collisions at  $\sqrt{s} = 13$  TeV
- **Covered analyses:**
  - Search for neutral LLPs from Higgs boson decays via VBF production [ATLAS-CONF-2023-051]
  - Search for dark photons in rare Z boson decays [arXiv:2306.07413]
  - Search for an ALP with forward proton scattering in association with photon pairs [arXiv:2304.10953]
  - Search for short- and long-lived ALPs in  $H \rightarrow aa \rightarrow 4\gamma$  decays with ATLAS [ATLAS-CONF-2023-040]
- **Other interesting results:**
  - Search for non-resonant production of semi-visible jets [arXiv:2305.18037]
  - Search for dark mesons decaying to top and bottom quarks [ATLAS-CONF-2023-021]
  - Search for resonant production of dark quarks in the di-jet final state [ATLAS-CONF-2023-047]

## Analysis overview & motivation

- Search for dark photons with masses in range of 0.1 - 15 GeV
- Using full LHC Run-2  $pp$  dataset ( $139 \text{ fb}^{-1}$ )
- Complements previous ATLAS searches in ggF and WH production channels
- Kinetic mixing parameter  $\varepsilon(\gamma_d, \gamma_{SM}) < 10^{-5}$  results in:
  - displaced decays of dark photons
  - dark-photon masses in  $\sim \text{MeV-GeV}$



$f_d$  = dark fermion  
 $\gamma_d$  = dark photon  
 $\gamma_{SM}$  = Standard Model (SM) photon  
**HLSP** = hidden lightest stable particle (stable dark fermion)



## Analysis strategy

### Muonic dark-photon jets ( $\mu$ DPJ)

- minimum 2 MS tracks; not matched to prompt muon candidates; no jets within  $\Delta R = 0.4$
- **cosmic-ray tagger**: DNN used to distinguish signal from cosmic-ray bkg; output  $> 0.5$ ; signal efficiency  $> 95\%$

### Calorimeter dark-photon jets (caloDPJ)

- single jets with low EMF with  $p_T > 20$  GeV and within  $|\eta| < 2.5$
- **QCD tagger**: CNN used to reduce fake caloDPJs arising from prompt jets; output  $> 0.5$ ; signal efficiency  $> 70\%$
- **BIB tagger**: CNN used to reject low EMF signatures in HCAL resulting from radiative losses by muons arising from BIB

## Event selection

- only leading DPJ used to classify the events as  $\mu$ DPJ or caloDPJ
- $\geq$  two jets with  $p_T \geq 30$  GeV
- $m_{jj} \geq 1000$  GeV
- $|\Delta\eta_{jj}| > 3$
- $|\Delta\phi_{jj}| < 2.5$  rad
- exactly 0 leptons
- exactly 0 b-tagged jets
- $E_T^{\text{miss}} \geq 100$  GeV

**DPJ** = dark-photon jets (collimated group of fermions)

**MS** = Muon Spectrometer

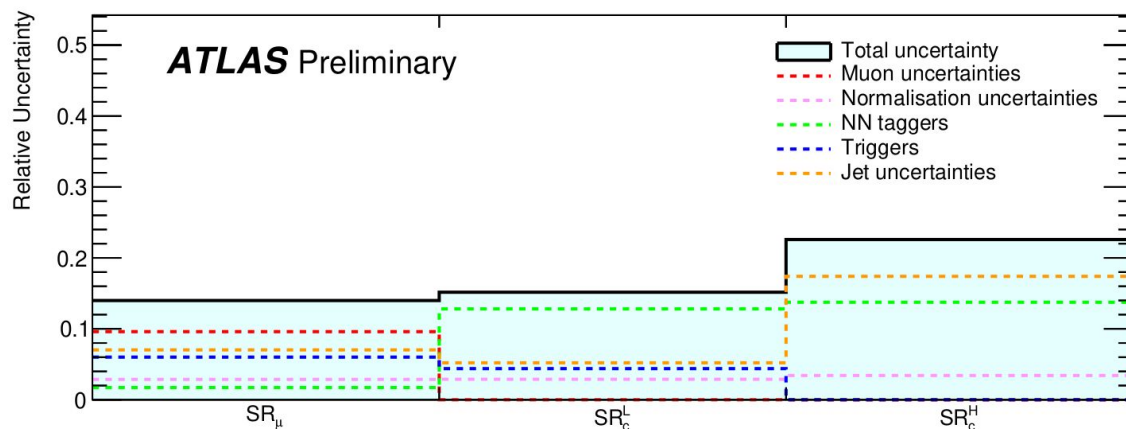
**EMF** (electromagnetic fraction) = ratio of the energy deposited in the EM calorimeter to the total jet energy

**BIB** = beam induced background

## Dominant backgrounds

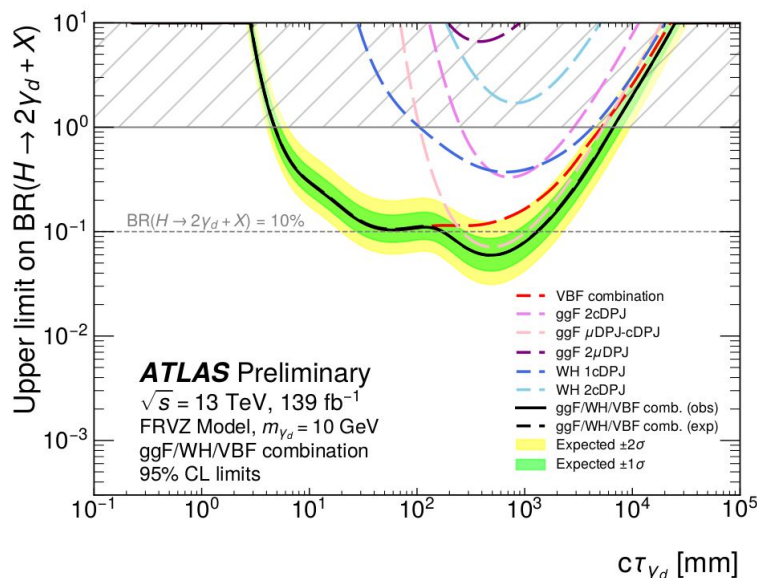
	$E_T^{\text{miss}}$ [GeV]	Main bkg process	Bkg estimation technique
$SR_\mu$	$> 100$	punch-through jets from rare multi-jet events	data-driven “ABCD” method
$SR_c^L$	[100, 225]	multi-jet and electroweak W and Z production	
$SR_c^H$	$> 225$		

## Systematic uncertainties

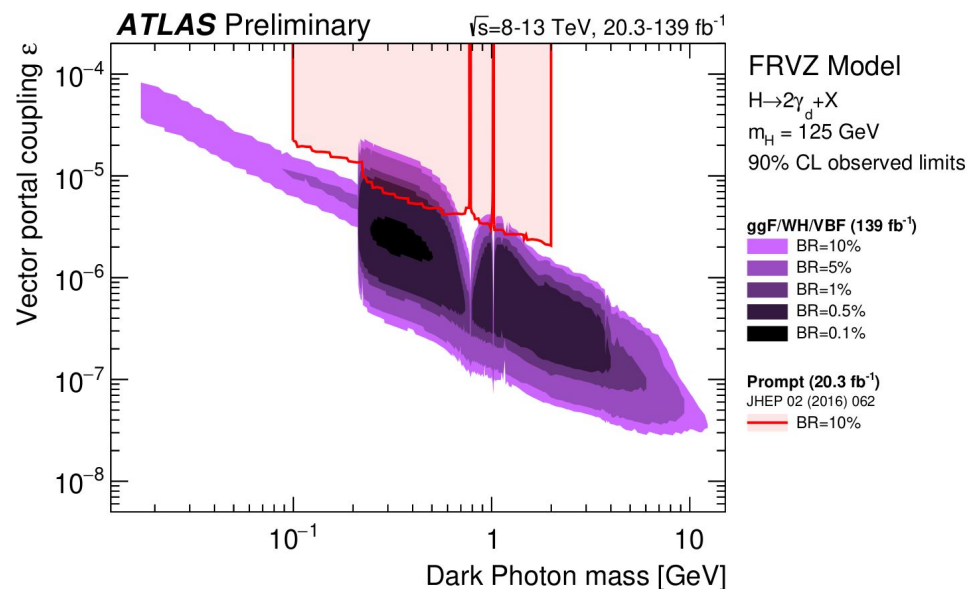


- Comparison of the relative uncertainty in the signal yield in each SR, showing the contributions from the different sources of uncertainty
- Averaged over different  $\gamma_d$  masses

## Analysis results



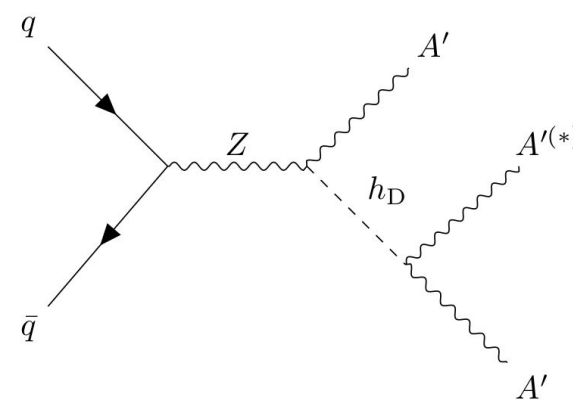
- Branching fractions above 10% can be excluded at 95% CL for  $H \rightarrow 2\gamma_d + X$  decays for dark photons with mean proper decay length between 173 and 1296 mm and mass of 10 GeV, a 34% (26%) **improvement** in the low (high) range compared to the previous search including only ggF and WH production modes.



- The 90% CL exclusion contours of the  $BR(H \rightarrow 2\gamma_d + X)$  as a function of the  $\gamma_d$  mass and  $\epsilon$
- Limits obtained assuming the SM cross-section for a 125 GeV Higgs boson and branching fractions between 0.1% and 10% for Higgs boson decays resulting in dark photons

## Analysis overview & motivation

- Search for dark photons with masses in range of 5 - 40 GeV except for the  $\Upsilon$  mass window [8.8, 11.1] GeV
- Using full LHC Run-2  $pp$  dataset ( $139 \text{ fb}^{-1}$ )
- Process:  $pp \rightarrow Z \rightarrow A' h_D \rightarrow A' A' A'^{(*)}$
- Kinetic mixing parameter  $\varepsilon(A', \gamma_{\text{SM}}) > 10^{-6}$  results in:
  - prompt decays of dark photons
- Hidden-sector gauge coupling  $\alpha_D$ : coupling of the  $A'$  to DS particles



$h_D$  = dark Higgs boson  
 $A'$  = dark photon which decays to SM fermions  
 $\gamma_{\text{SM}}$  = Standard Model (SM) photon

## Event selection

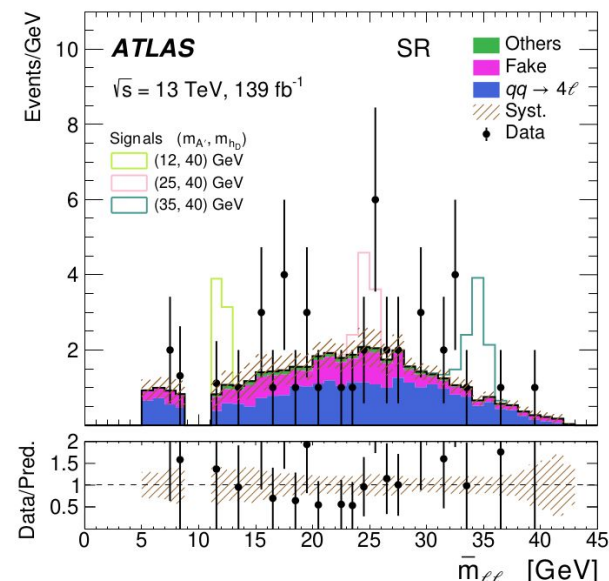
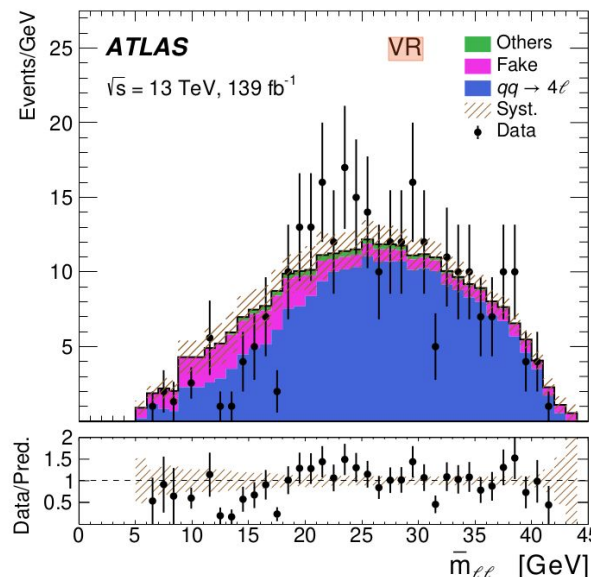
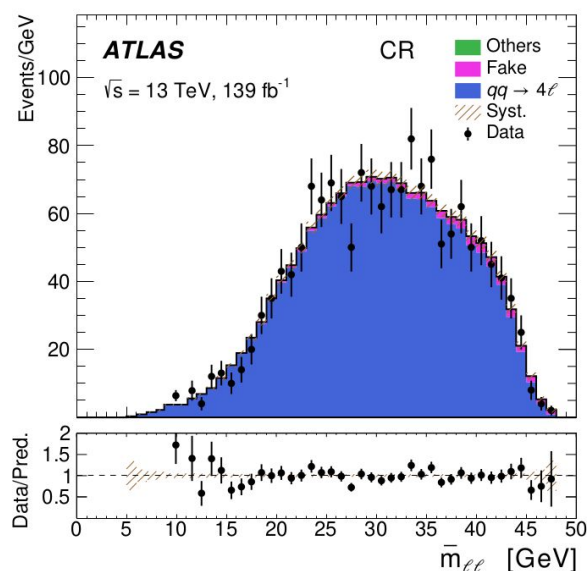
- muon candidates:  $p_T > 15$  GeV; electron candidates:  $p_T > 4.5$  GeV
- $\geq$  two same-flavour and opposite-charge (SFOC) lepton pairs
- $m_{4\ell} < m_Z - 5$  GeV to suppress the SM  $pp \rightarrow 4\ell$  background
- the lepton quadruplet is selected such that  $|m_{\ell^+\ell^-} - m_{\ell'^+\ell'^-}|$  is minimal
- $m_{\ell_3\ell_4}/m_{\ell_1\ell_2} > 0.85$  to ensure both originate from an  $A'$  decay
- same- (different-) flavored leptons are required to have an angular separation of  $\Delta R > 0.1$  (0.2)
- $m_{\ell^+\ell^-} > 5$  GeV

## Background contribution

- Dominant bkg in SR:  $qq \rightarrow 4\ell$  process
- CR:  $m_Z - 5$  GeV  $< m_{4\ell} < m_Z + 5$  GeV; VR: same as SR but  $m_{\ell_3\ell_4}/m_{\ell_1\ell_2} < 0.85$
- Subleading bkg: from processes involving the production of Z+jets, top-quark and W Zjj events, with non-prompt leptons from hadron decays or misidentification of jets
- $pp \rightarrow H \rightarrow 4\ell$ , the  $gg \rightarrow ZZ \rightarrow 4\ell$  continuum, and triboson and  $ttZ$  processes  $< 5\%$

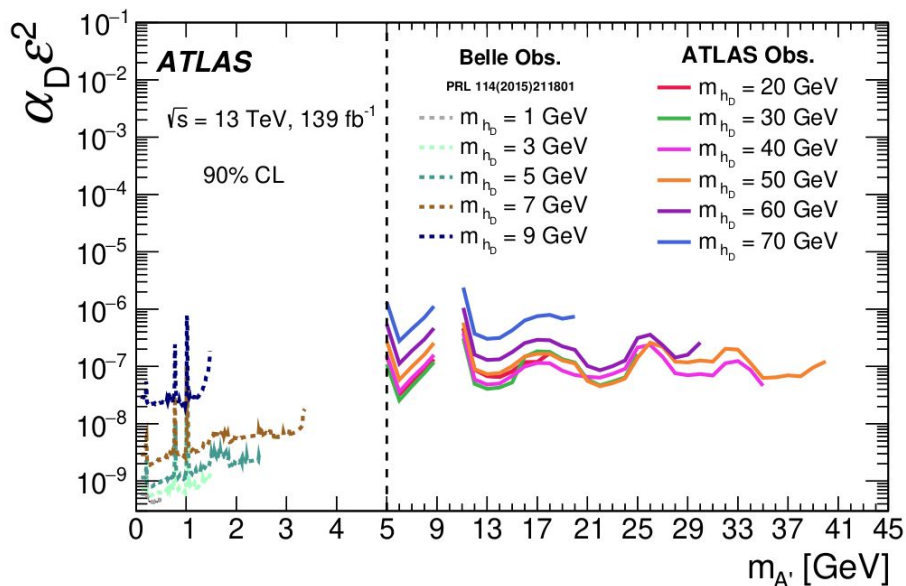


## Expected background and observed data yields

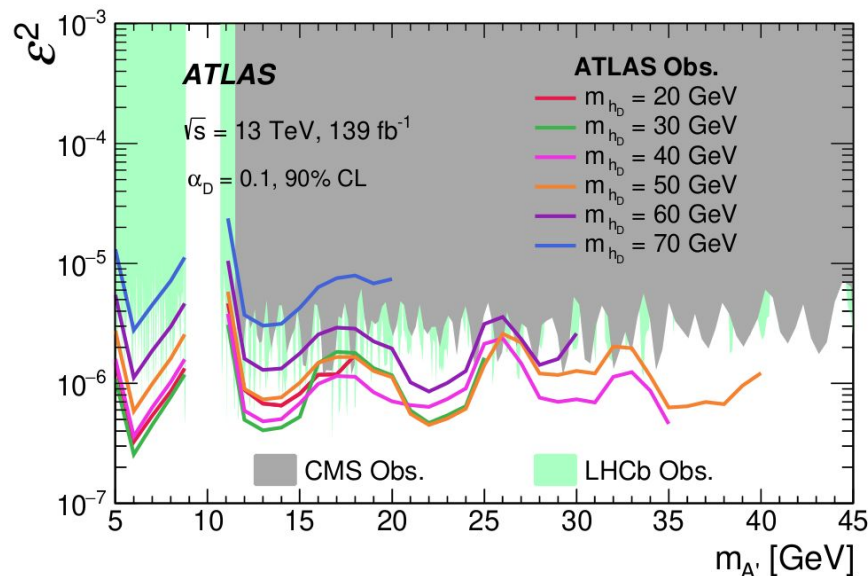


- Data found to be consistent with the background expectation in all three regions
- No significant deviation from the SM background hypothesis is observed

## Analysis results



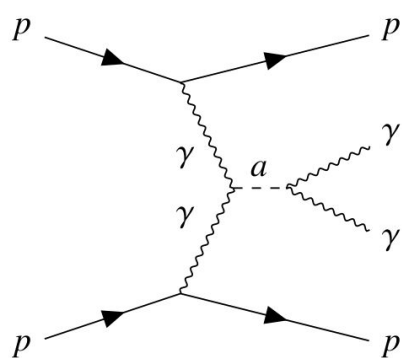
- Observed 90% CL upper limits on  $\alpha_D \varepsilon^2$ , as a function of  $m_{A'}$ , with different  $m_{h_D}$  masses
- The search is sensitive to a set of  $m_{A'}$  and  $m_{h_D}$  masses complementary to those in a similar search reported by the [Belle Collaboration](#)



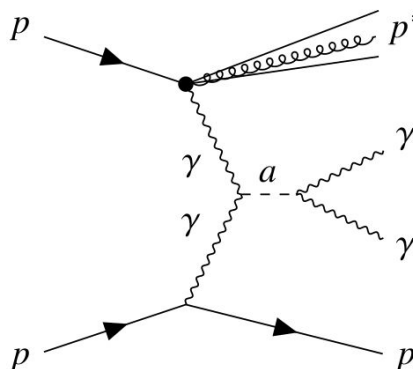
- Observed 90% CL upper limits on  $\varepsilon^2$ , assuming of  $\alpha_D = 0.1$ , as a function of  $m_{A'}$ , with  $20 \text{ GeV} < m_{h_D} < 70 \text{ GeV}$
- For  $m_{h_D} \lesssim 60 \text{ GeV}$  and  $\alpha_D \gtrsim 0.1$ , the **exclusion sensitivity of this search is comparable to, or better than, that of the [LHCb](#) and [CMS](#) searches**

## Analysis overview & motivation

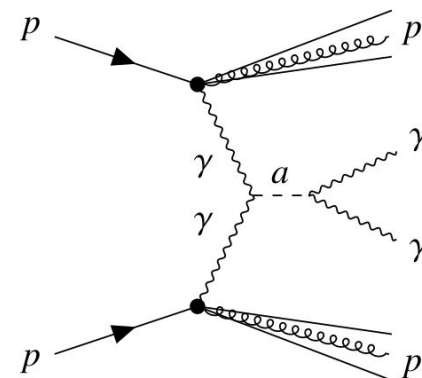
- Covering diphoton-mass range of 150 - 1600 GeV
- Using  $14.6 \text{ fb}^{-1}$  of data collected in  $pp$  collisions at  $\sqrt{s} = 13 \text{ TeV}$
- Pair of outgoing photons detected in the central detector around IP while scattered protons are detected by ATLAS Forward Proton (AFP) spectrometer system ([proton tagging](#))



exclusive light-by-light scattering

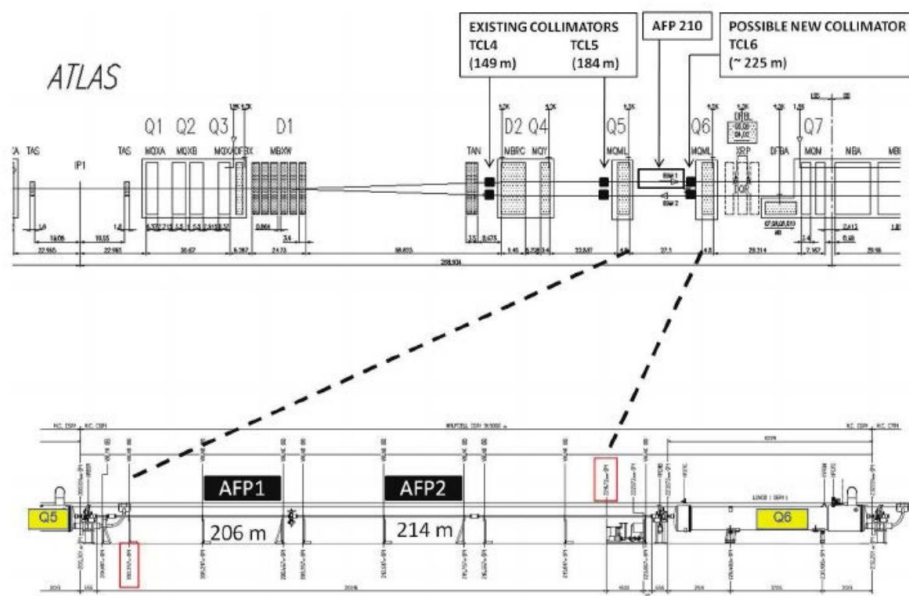


single-dissociative (SD) light-by-light scattering



double-dissociative (DD) light-by-light scattering

## Experimental setup



- ATLAS Forward Proton (AFP) spectrometer system: Roman Pot systems used to detect forward scattered protons
- 4 tracking units located at  $z = \pm 205$  m (Near station) and  $\pm 217$  m (Far station); each pair on A and C side
- Protons transported to the AFP by the beamline magnets leave hits in its silicon trackers  $\Rightarrow$  processed by per-plane clustering and per-station track-finding algorithms  $\Rightarrow$  tracks are reconstructed from clusters found in at least two planes in each station

## Event selection

### ATLAS ECAL

- $\geq 2$  photon candidates with  $p_T > 40$  GeV and  $|\eta| < 2.37$ , excluding  $1.37 < |\eta| < 1.52$
- azimuthal misalignment between the pair of photons was required to be small, as determined by an acoplanarity  $A_\phi^{\gamma\gamma} = 1 - |\Delta\phi_{\gamma\gamma}|/\pi < 0.01$

### AFP

- Track spatial coordinates  $\Rightarrow$  proton energy and momentum at the IP, using the known beam optics  $\Rightarrow$  reconstruction:

**fractional energy loss of the scattered proton:**  $\xi_{\text{AFP}} = 1 - E_{\text{scattered}}/E_{\text{beam}}$

**$\xi$  using the kinematics of the central photon pair:**  $\xi_{\gamma\gamma}^\pm = (m_{\gamma\gamma}/\sqrt{s}) e^{\pm\eta_{\gamma\gamma}}$

- Proton-tagged diphoton pairs required on at least one AFP side (forward-proton matching):

$$|\Delta\xi| = \xi_{\text{AFP}} - \xi_{\gamma\gamma} < \xi_{\text{th}} ; \xi_{\text{th}} = 0.004 + 0.1\xi_{\gamma\gamma}$$

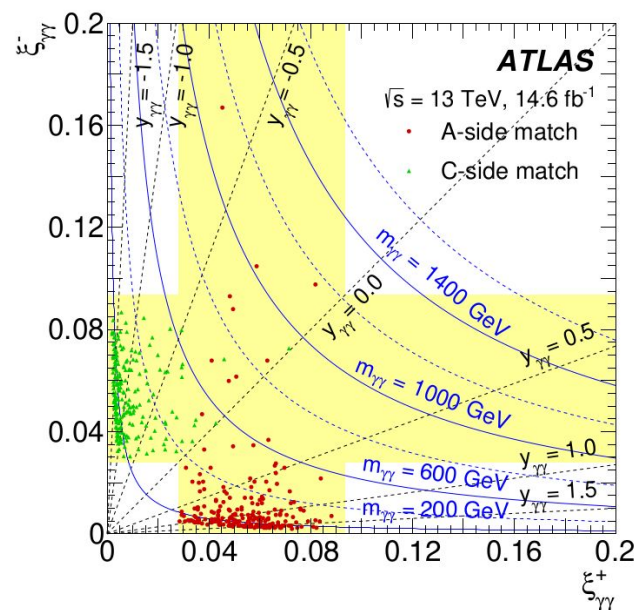


## Selection efficiency

- A total of 441 events observed in range  $150 < m_{\gamma\gamma} < 1600$  GeV
- 219 (222) events passed the matching selection for the A(C)-side
- No event passed the matching requirement for both the A-side and C-side

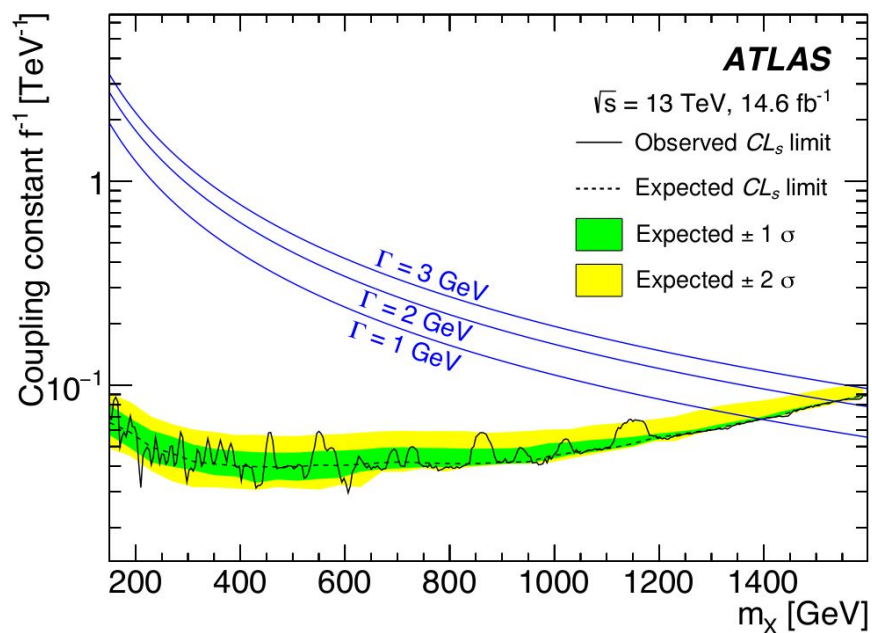
## Dominant backgrounds

- Combinatorial backgrounds: pair of photons (or hadronic jets misidentified as photons) produced in a  $pp$  interaction other than that giving the detected forward protons but within the same bunch crossing
- single-vertex backgrounds:  $\gamma\gamma \rightarrow \ell^+\ell^-$ ,  $\gamma\gamma \rightarrow \gamma\gamma$ , gluon-initiated central exclusive production (CEP)

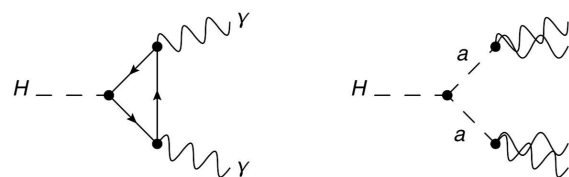


## Analysis results

- Inferred upper limit on the ALP coupling constant, assuming a 100% decay branching ratio into two photons: in the range 0.04 – 0.09  $\text{TeV}^{-1}$  at 95% CL
- Results **comparable to those of the CMS-TOTEM collaboration** and **extending** their measured mass range to lower values



## Analysis motivation

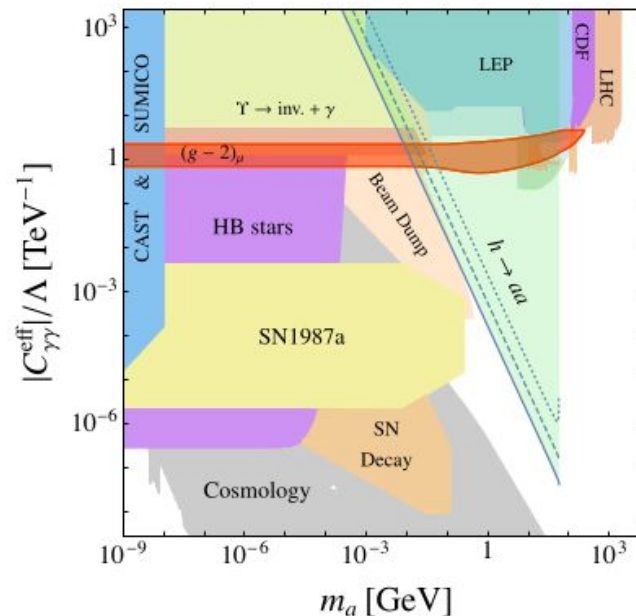


- Probing unconstrained  $m_a - C_W$  parameter space:
  - $(gg)H \rightarrow aa \rightarrow \gamma\gamma\gamma$
  - $100 \text{ MeV} \leq m_a \leq 62 \text{ GeV}$
  - $1e-5 \leq C_W \leq 1$

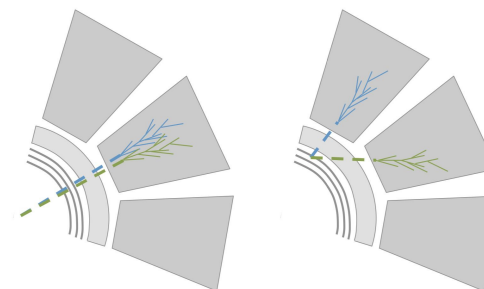
## Challenges

- ALPs with long lifetimes can decay close to ECAL
- Requiring that axions decay within ECAL ( $< 1970 \text{ mm}$ )

$$\Gamma_{a\gamma\gamma} = \frac{4\pi\alpha^2 m_a^3}{\Lambda^2} |C_{a\gamma\gamma}|^2$$



M. Bauer, M. Neubert, and A. Thamm, J. High Energ. Phys. 2017, 44 (2017)



- **Photon ID** based on 2 NNs (each with 2 hidden layers - 7 and 5 nodes; with shower shapes used as input variables):

**NN1: real vs. fake photons**

- Signal:  $H \rightarrow aa$ ,  $H \rightarrow \gamma\gamma$
- Background: selected data with photons such that  $p_T > 15$  GeV, fail loose ID, isolated ( $ETCone40/p_T < 0.1$ ),  $m_{inv} > 60$  GeV (Higgs region excluded)

**NN2: merged vs. single photons**

- Signal:  $H \rightarrow aa \rightarrow \gamma\gamma\gamma\gamma$  merged photons
- Background:  $H \rightarrow aa \rightarrow \gamma\gamma\gamma\gamma$  single photons

- Each photon gets one of 3 labels:
  - merged ( $ANN1 > 0.98$ ,  $ANN2 > 0.5$ ,  $!tight$ )
  - loose
  - tight

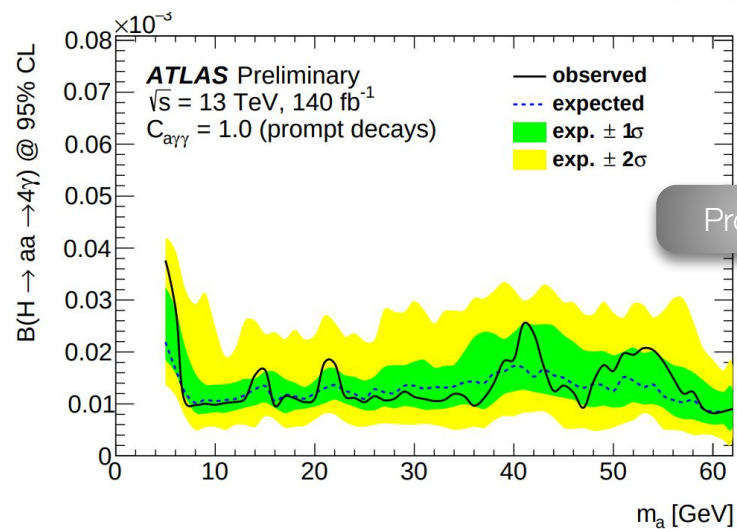
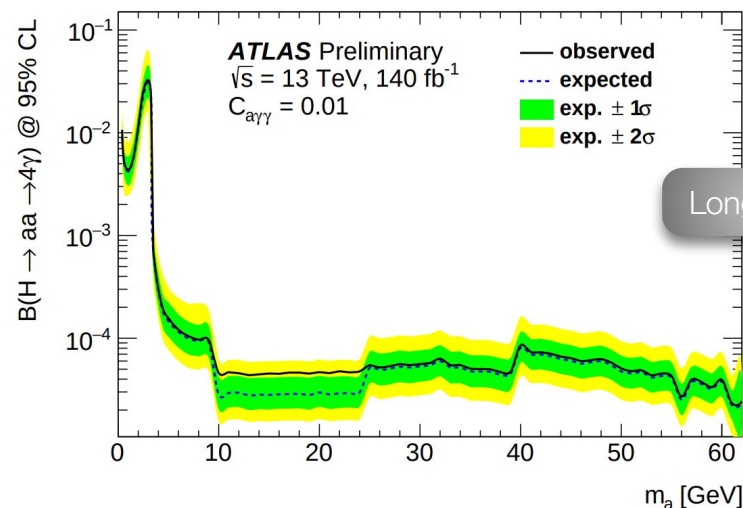
- Resulting in 5 categories:
  - **4S**: 4 loose photons, at least 1 ( $\geq 3$ ) tight photon
  - **3S**: 2 tight + 1 loose photons
  - **2M**: 2 merged photons
  - **1M1S**: 1 merged + 1 loose photon
  - **2S**: 2 tight photons (dominated by  $H \rightarrow \gamma\gamma$  background)
  
- **Axion mass reconstruction**: only possible in 3S and 4S categories; used to define SR and CR (by inverting the axion mass requirement)
- 2 NNs for each case:
  - Input:  $m_{\text{inv}}$  of all possible di-photon combinations, pairwise differences in  $p_T$ , pairwise differences in direction
  - Labels based on MC truth information

**Prompt analysis (4S<sub>p</sub>)**: more stringent categorization criteria (loosened needed for long-lived case as ID efficiency drops for axions decaying closer to the ECal)

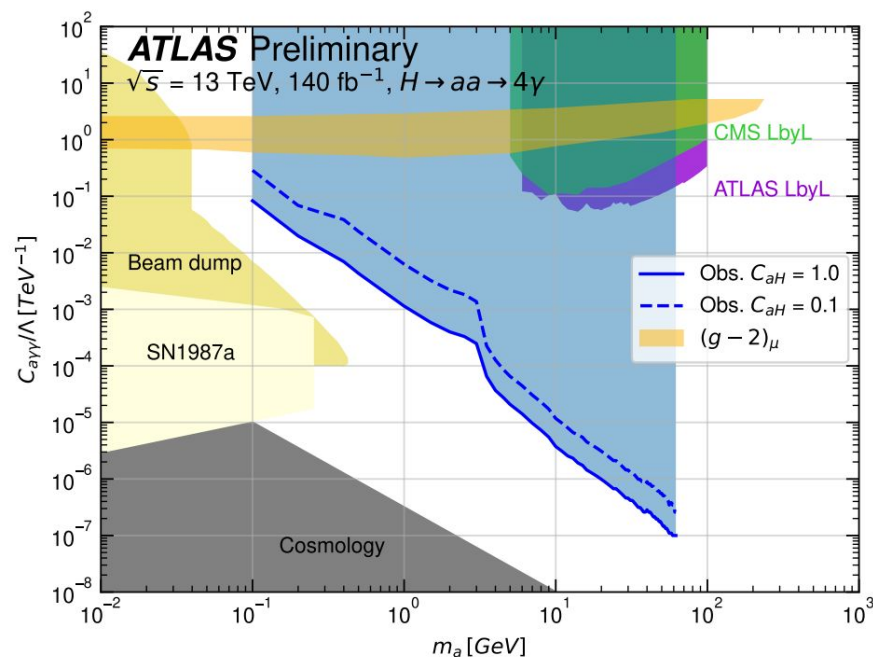


## Limits

- Setting upper limits on  $B(H \rightarrow aa \rightarrow 4\gamma)$  at 95% CL as a function of the axion mass and for different ALP-photon couplings
- The long-lived searches significantly less sensitive than the prompt searches due to the looser signal selection and consequently larger background contributions
- The observed limits agree well with the expected limits



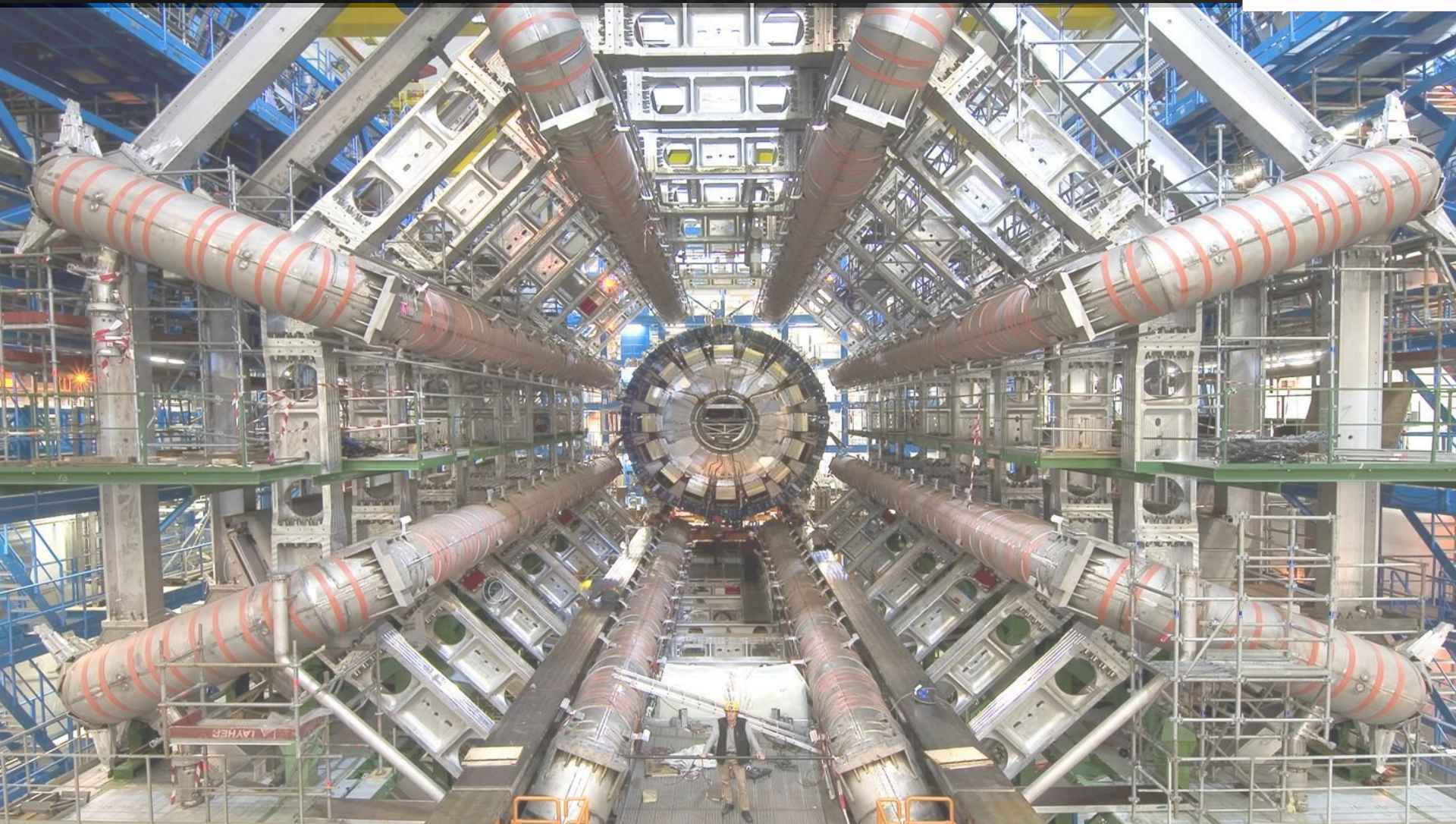
- Limits on ALP masses with  $m_a > 15$  GeV:
  - ~ one order of magnitude more stringent than previous ATLAS analyses using 8 TeV data
  - similar to slightly better sensitivity as previous analyses from CMS using  $132 \text{ fb}^{-1}$  of  $\sqrt{s} = 13$  TeV data
- First limits on ALPs with masses  $< 10$  GeV derived at ATLAS
  - 40% more stringent compared to the previous results from CMS using  $136 \text{ fb}^{-1}$  of  $\sqrt{s} = 13$  TeV
- **Most stringent limits to date**
- Excluded most of the remaining parameter space that could explain the  **$(g-2)_\mu$  discrepancy**



Limits on the ALP mass and coupling to photons at 95% CL, assuming  $|C_{a\gamma\gamma}^{eff}/\Lambda^2| = 1 \text{ TeV}^{-2}$  (solid line) and  $|C_{aH}^{eff}/\Lambda^2| = 0.1 \text{ TeV}^{-2}$  (dashed line)

- **Search for neutral LLPs from Higgs boson decays via VBF production**  
[ATLAS-CONF-2023-051]: 34% (26%) improvement in the low (high) range compared to the previous search including only ggF and WH production modes
  - **Search for dark photons in rare Z boson decays** [arXiv:2306.07413]: results complementary to, and higher than, results by the [Belle Collaboration](#); exclusion sensitivity comparable to, or better than, results by [LHCb](#) and [CMS](#) searches
  - **Search for an ALP with forward proton scattering in association with photon pairs**  
[arXiv:2304.10953]: comparable to results by [CMS-TOTEM collaboration](#) and extending their measured mass range to lower values
  - **Search for short- and long-lived ALPs in  $H \rightarrow aa \rightarrow 4\gamma$  decays with ATLAS**  
[ATLAS-CONF-2023-040]: First limits on ALPs with masses  $< 10$  GeV derived at ATLAS; 40% more stringent compared to the previous results from CMS using  $136 \text{ fb}^{-1}$  of  $\sqrt{s} = 13$  TeV
- 
- ATLAS focuses on furthering the searches for BSM physics
  - More theoretical models needed

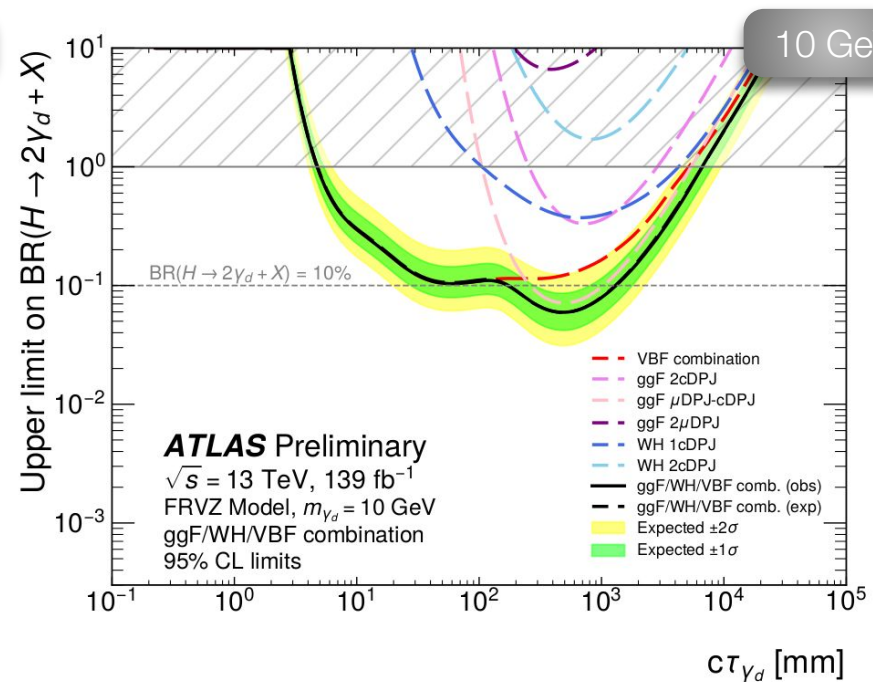
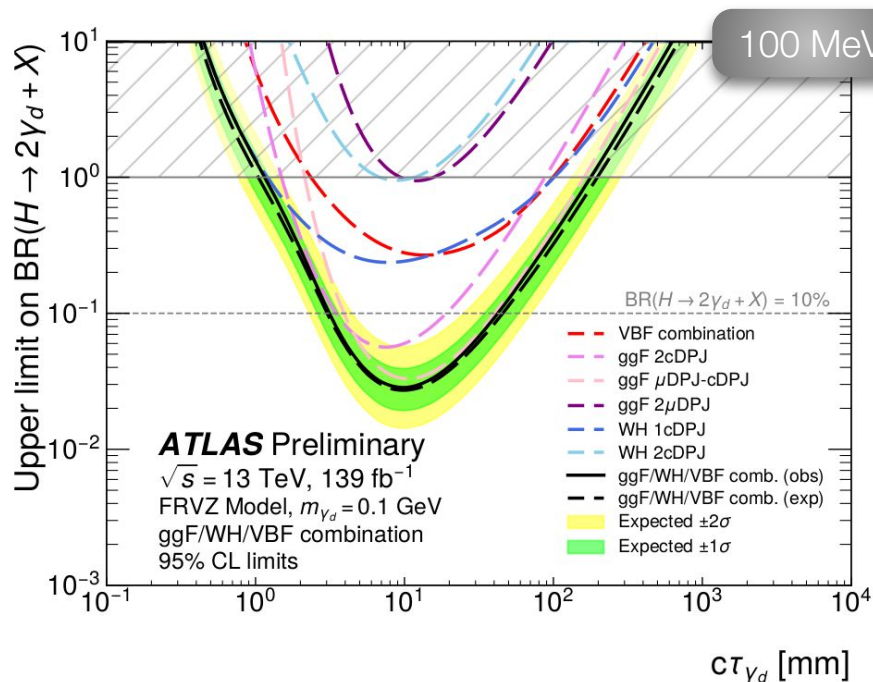






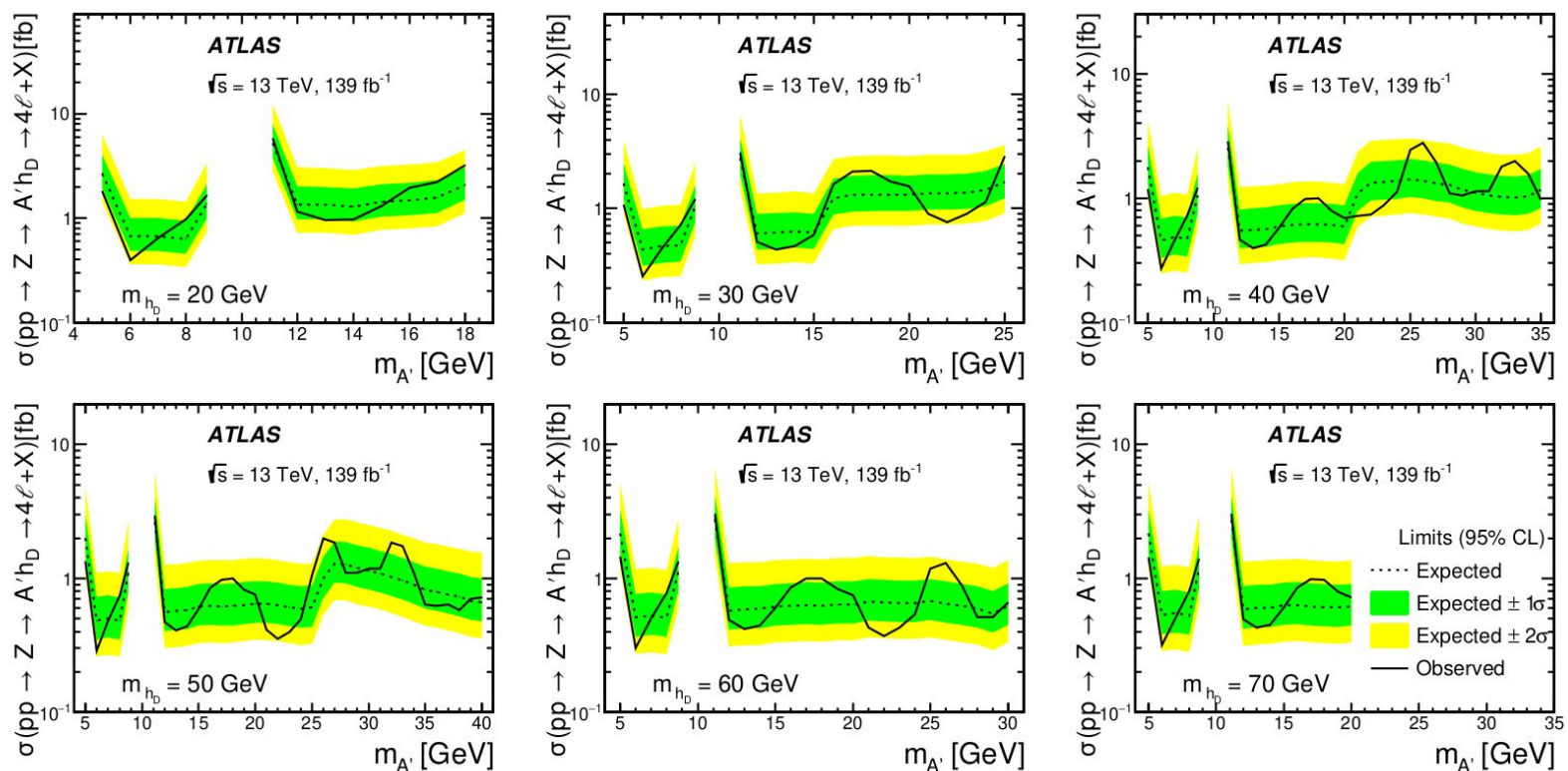
[ATLAS-CONF-2023-051]

## Analysis results



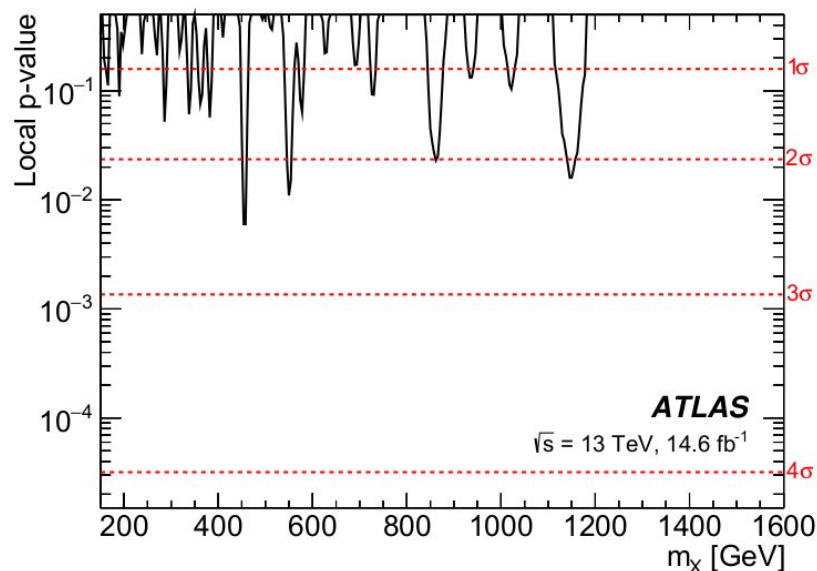


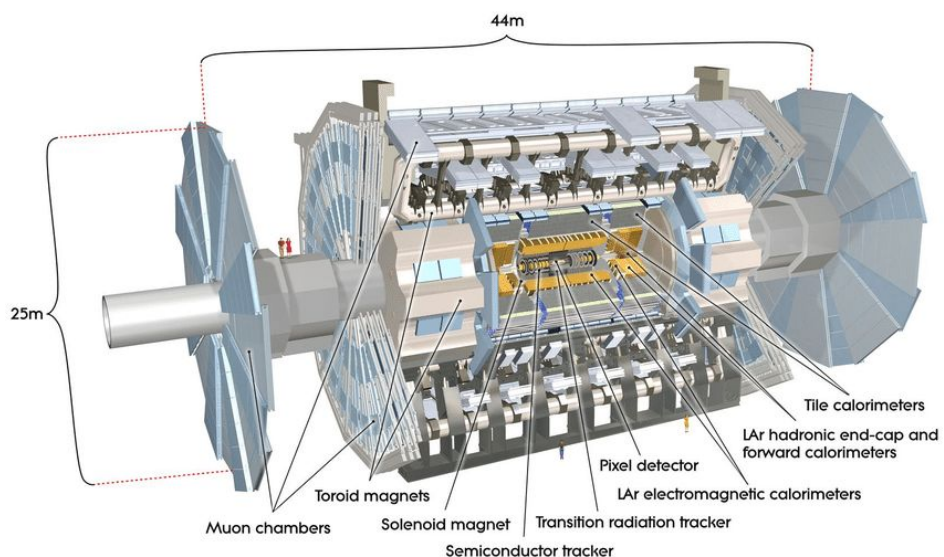
## Observed and expected upper limits



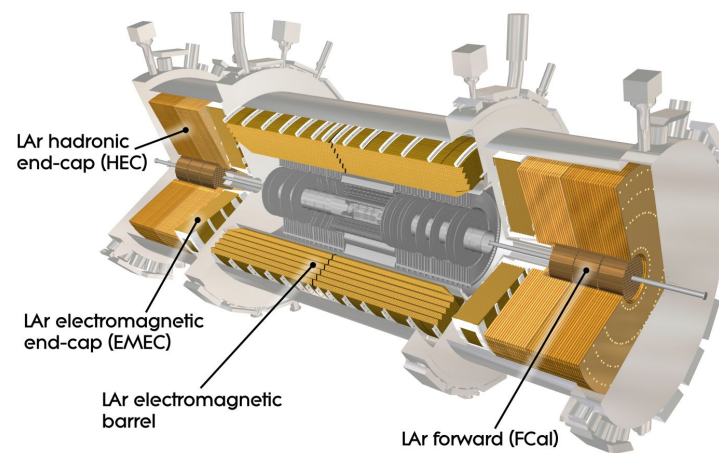
## Statistical procedure

- The probability of compatibility with the background-only hypothesis, quantified as the local  $p$ -value, is shown as a function of the hypothesised ALP resonance mass
- The most significant excess, observed at  $m_X = 454$  GeV, has a local significance of  $2.51\sigma$
- The global  $p$ -value for the null hypothesis is larger than 0.5, from which it is concluded that no significant excess over the background-only hypothesis is observed





## Calorimeter system



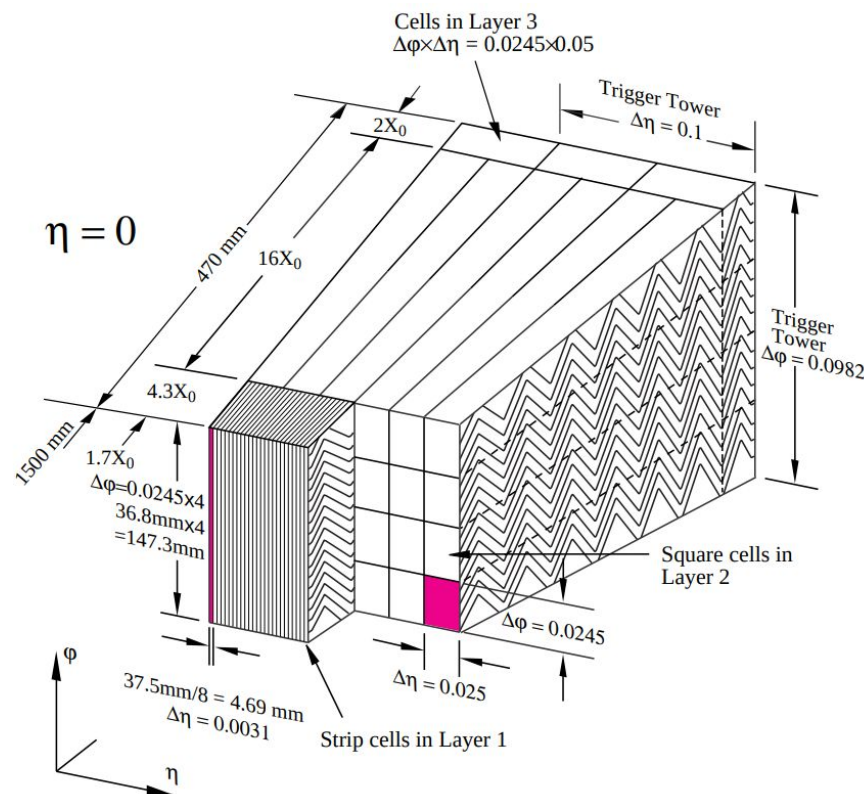
- Liquid argon calorimeter (LAr)

- specially designed to identify electrons and photons; honeycomb pattern
- kept at  $-184^{\circ}\text{C}$
- features layers of metal (either tungsten, copper or lead) that absorb incoming particles, converting them into a “shower” of new, lower energy particles, which ionise liquid argon sandwiched between the layers, producing an electric current that is measured

[ATLAS-CONF-2023-040]

- 9 discriminating variables (DVs) based on energy in cells of ECAL and leakage in hadronic calorimeter HCAL
  
- Loose ID:
  - exploits the DVs in the HCAL and in the ECAL middle layer
  - used by triggers or as background control region
  
- Tight ID:
  - tighter cuts on DVs than the ones used by Loose ID
  - using also ECAL strip layer
  - used for offline analysis

- Sketch of a barrel module with the granularity of cells depicted in  $\eta$  and  $\phi$





- 9 discriminating variables (DVs) based on energy in cells of ECAL and leakage in hadronic calorimeter HCAL

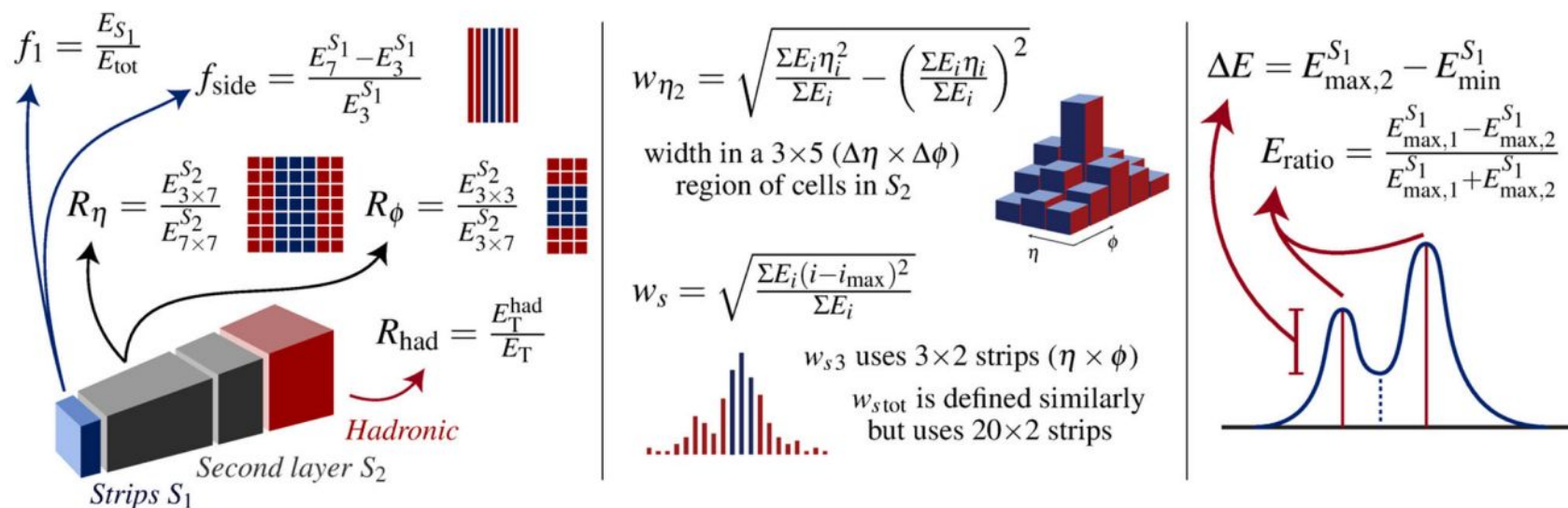


**Fig. 2** Schematic representation of the photon identification discriminating variables, from Ref. [23].  $E_C^{S_N}$  identify the electromagnetic energy collected in the  $N$ -th longitudinal layer of the electromagnetic

calorimeter in a cluster of properties  $C$ , identifying the number and/or properties of selected cells.  $E_i$  is the energy in the  $i$ -th cell,  $\eta_i$  the pseudorapidity centre of that cell



## Event selection

- Preselection:
  - diphoton triggers
  - $\geq 1$  reconstructed PV
  - $> 2$  photons with  $p_T > 15$  GeV and  $|\eta| < 2.37$  (calo crack excluded)
  - track based isolation:  $p_T^{\text{cone20}}/p_T < 0.05$

## 2-photon final states

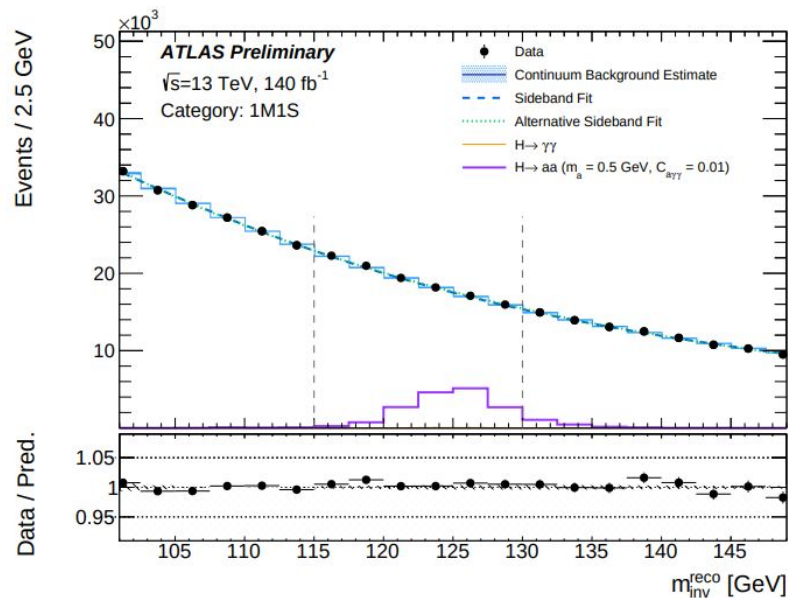
- Using a sideband in  $m_H$  distribution to fit the background contribution in  $[100, 150]$  GeV, excluding signal region
- Used fit functions:
  - 2S and 1M1S: Landau
  - 2M: Polynomial of 3rd order
- Cross-checks:
  - 2 $\gamma$  QCD MC
  - data driven: inverted isolation cut

## 3- and 4-photon final states

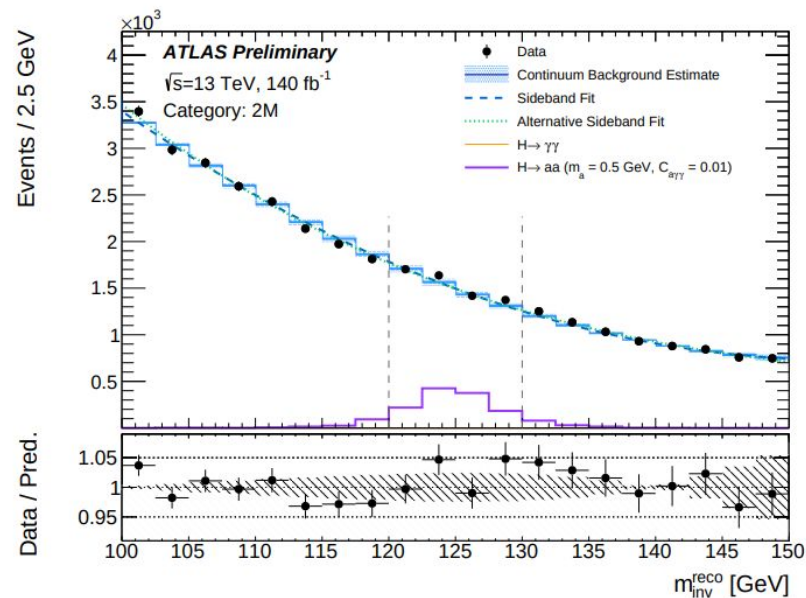
- Using a sideband in  $m_H$  distribution to fit the background contribution in  $[85, 150]$  GeV and  $[90, 150]$  GeV for 3S and 4S respectively, excluding signal region
- Used fit functions:
  - Polynomial of 3rd order
- Cross-checks:
  - 3 $\gamma$ , 4 $\gamma$  QCD MC
  - data driven: inverted axion mass requirement

## Prompt final states

- Considering only 4S case with  $m_A > 5$  GeV; low statistics due to harsher rejection of fake photon signatures
- Using a 2D sideband fit approach with the  $m_H^{\text{reco}}$  vs.  $m_a^{\text{reco}}$  spectra with SR and CR defined as:
  - SR:  $120 \text{ GeV} < m_H < 130 \text{ GeV}$  and  $m_a$  in  $m_a \pm \text{stepsize}$
  - CR1:  $110 \text{ GeV} < m_H < 140 \text{ GeV}$  and  $m_a$  in  $m_a \pm \text{stepsize} * 1.5$
  - CR2:  $105 \text{ GeV} < m_H < 145 \text{ GeV}$  and  $m_a$  in  $m_a \pm \text{stepsize} * 2.5$
- Background estimated as an average of data events in the CR

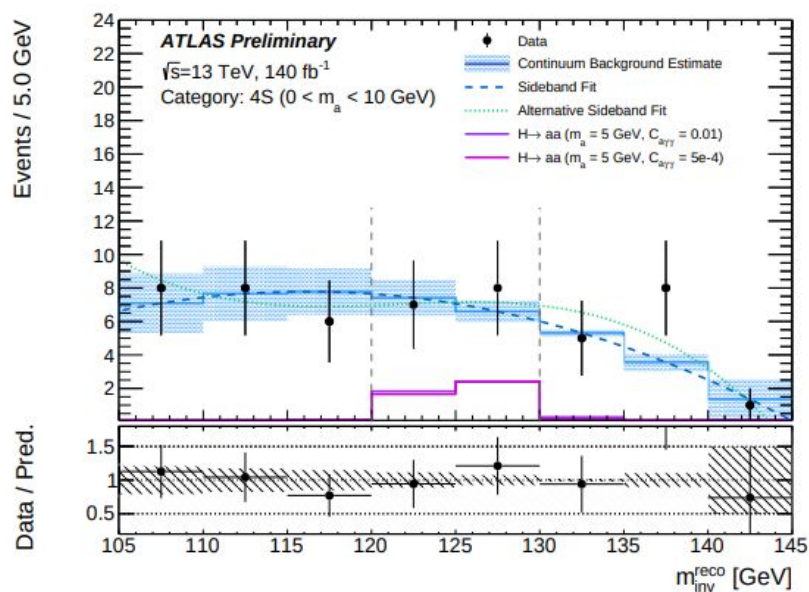


(a)

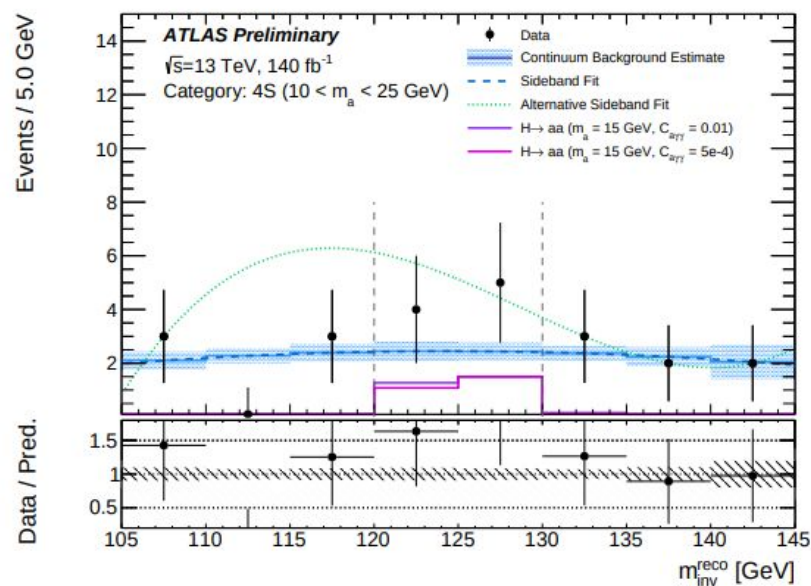


(b)

Figure 1:  $m_{\text{inv}}^{\text{reco}}$  distribution for the nominal signal selection for the (a) 1M1S, and (b) 2M category. The nominal sideband fitting function as well as its systematic variation is shown for both cases. The expected signal shape for  $C_{a\gamma\gamma} = 0.1$  is also shown with an arbitrary normalization. The signal region selection on  $m_{\text{inv}}^{\text{reco}}$  is indicated as dashed lines.

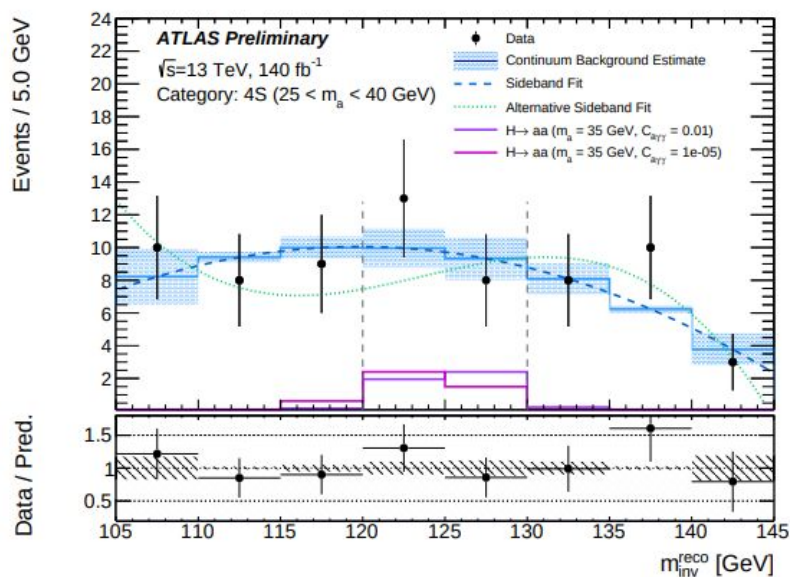


(a)

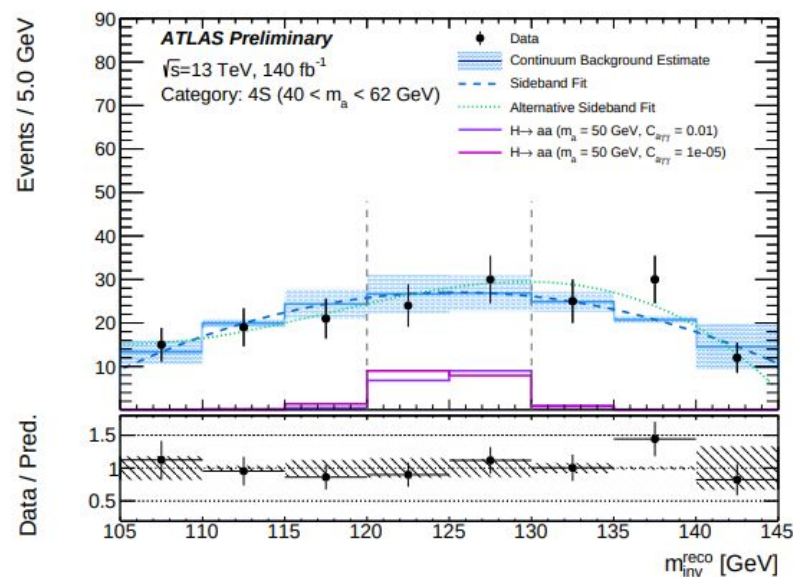


(b)





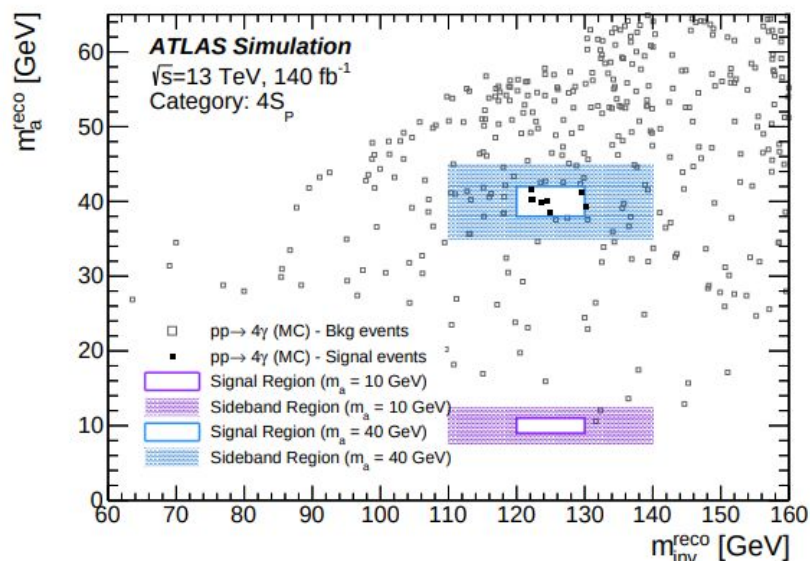
(c)



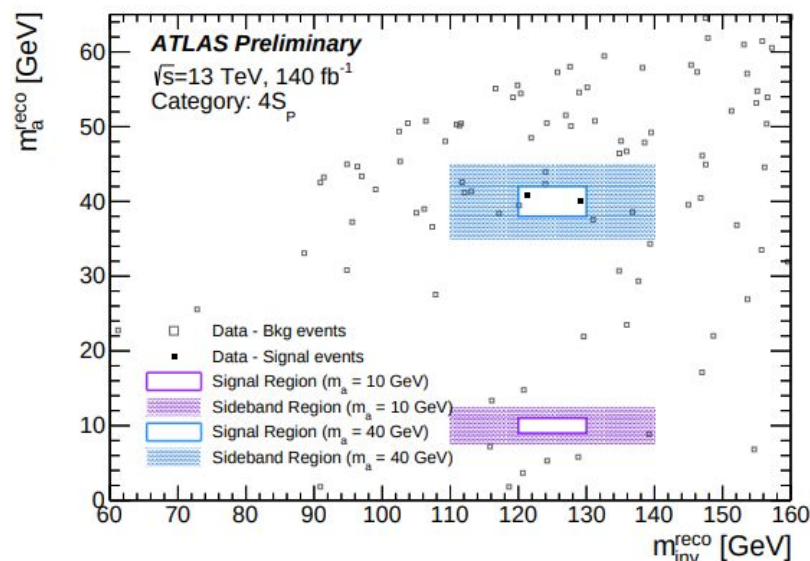
(d)

Figure 2: 4S category in the search for long-lived ALPs:  $m_{\text{inv}}^{\text{reco}}$  distribution for the nominal signal selection including the nominal and alternative sideband fitting functions, the estimated background from the sideband fit in the signal region as well as the expected signal shape for two ALP-photon couplings with arbitrary normalization. The 4 plots show different ALP mass ranges: (a)  $0 < m_a < 10$  GeV, (b)  $10 < m_a < 25$  GeV, (c)  $25 < m_a < 40$  GeV, (d)  $40 < m_a < 62$  GeV. The signal region selection on  $m_a^{\text{reco}}$  is applied while the signal region selection on  $m_{\text{inv}}^{\text{reco}}$  is indicated as dashed lines.





(a) MC

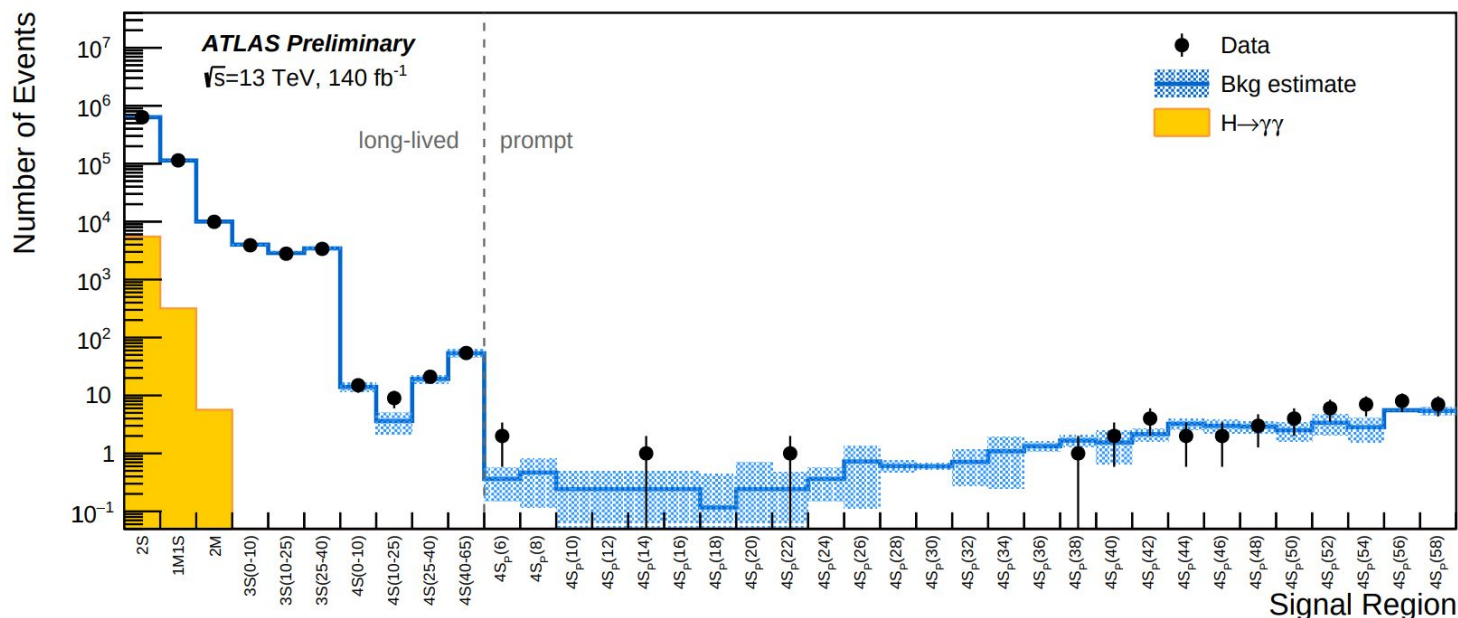


(b) Data

Figure 3:  $m_{\text{inv}}^{\text{reco}}$  vs.  $m_a^{\text{reco}}$  for the  $4S_P$  categories in the search for promptly decaying ALPs, for (a) simulated  $pp \rightarrow 4\gamma$  sample and (b) for data. The signal (sideband) regions are indicated as solid lines (shaded areas) for the searches for ALPs with masses of 10 and 40 GeV.

[ATLAS-CONF-2023-040]

- Overview of estimated background events compared to measured data events in the signal region of the most sensitive categories
- The  $H \rightarrow \gamma\gamma$  background is only visible in the first three bins, corresponding to the 2-photon categories



[ATLAS-CONF-2023-040]

## Nominal uncertainties

- Nominal (as recommended) systematic uncertainties are evaluated for:
  - Lumi 0.8%
  - Pileup < 1%
  - Trigger 2% - 3%
  - Photon ID, ISO, scale, resolution  $\leq 3\%$  on selected events

**Real vs. fake:** 3%  
**Merged vs. resolved:** 4% to 15%  
**Loose ID:** 7% to 23%  
**Tight ID:** 6% to 21%

## Custom uncertainties

- Special attention paid to the systematic uncertainties due to displaced vertices and their effect on the shower shapes
  - Using cluster shapes associated to tracks from displaced vertices of long lived hadrons (kaons) - data and MC
  - 3 regions:
    - **near:**  $z_0 < 20$  mm,  $d_0 < 1$  mm
    - **medium:**  $20$  mm  $< z_0 < 500$  mm,  $1$  mm  $< d_0 < 80$  mm
    - **far:**  $500$  mm  $< z_0$ ,  $d_0 > 80$  mm
  - The dependence of the mean and RMS of the shower shape distribution on the decay length fitted by a polynomial
  - Applied to photon clusters in our signal MC; ID/classification efficiency recalculated after shower shape fudging
- NN classifiers:
- $Z \rightarrow ee$  events used comparing MC and data, electron shower shape variables used as inputs
  - Difference propagated through analysis: up to 15% normalisation uncertainty in the 2M and 1M1S categories